This is the author's accepted version of the article. The final version published by IEEE is S. Bakirtzis, I. Wassell, M. Fiore and J. Zhang, "Stochastic Evaluation of Indoor Wireless Network Performance with Data-Driven Propagation Models," IEEE GLOBECOM 2022 - IEEE Global Communications Conference, 2022, pp. TBD, doi: TBD.

Stochastic Evaluation of Indoor Wireless Network Performance with Data-Driven Propagation Models

Stefanos Bakirtzis, Ian Wassell
Ranplan Wireless
Dept. of Computer Science and Technology
University of Cambridge
Cambridge, United Kingdom
ssb45@cam.ac.uk, ijw24@cam.ac.uk

Marco Fiore
IMDEA Networks Institute
Madrid, Spain
marco.fiore@imdea.org

Jie Zhang
Ranplan Wireless
Dept. of Electronic and Electrical Engineering
The University of Sheffield
Sheffield, United Kingdom
jie.zhang@sheffield.ac.uk

***Abstract*—Cell densification through the installation of small-cells and femtocells in indoor environments is an emerging solution to enhance the operation of wireless networks. The deployment of new components within the heart of the radio access network calls for expedient tools that assist and ensure their optimal placement within the existing network infrastructure. In this paper, we introduce metrics that can characterize indoor wireless network performance (IWNP) in terms of coverage and capacity, and we evaluate them via physics-based propagation models. In particular, we exploit a deterministic propagation model, i.e., a ray-tracer, as well as a novel machine learning-based propagation model. We demonstrate that data-driven propagation models can be leveraged for the rigorous evaluation of the IWNP metrics, yielding a remarkable computational efficiency compared to the conventional deterministic models. The use of physics-based site-specific propagation models allows for the particularities of each indoor geometry to be taken into account, and also makes feasible the consideration of uncertainties related to the indoor environment. In this case, the IWNP metrics are expressed as stochastic quantities and a stochastic solution is derived through an efficient polynomial chaos expansion representation, enabling on-the-fly computation of the IWNP metrics statistics.**

***Index Terms*—Radio propagation, machine learning, indoor communications, uncertainty quantification, ray tracing, 5G.**

I. Introduction

Fifth-generation (5G) mobile networks are anticipated to revolutionize the structure of the wireless ecosystem. In addition to the standard services provided by legacy communication systems, 5G systems will support a set of highly heterogeneous services. Hence, they are expected to handle a substantially larger volume of mobile traffic with diverse requirements in terms of bandwidth, throughput, latency, quality of service and reliability. Remarkably, although the preponderance of this traffic is generated in indoor environments [1], the largest part of the legacy communication systems radio access network is deployed outdoors.

To enhance the performance of the wireless network and reduce the capital expenditure and operating expenses, lately the interest of mobile network operators (MNOs) has been steered towards the deployment of pico and femto cells in indoor environments [2]. Indeed, cell densification can improve wireless coverage, increase network's capacity by offloading existing wireless traffic, and enhance users' quality of experience. Due to resource and budget constraints, MNOs will deploy 5G indoor networks in a phased and orderly manner. The appropriate building and network topology selection requires robust and reliable tools and metrics that will be able to assess the performance of an indoor wireless network, and consequently guide its optimal design.

An important effort towards this directions was made in [3], [4], where the authors introduced the idea of building wireless performance (BWP), which emerges as a fundamental utility of a building, similarly to its eco-friendliness and its electricity, water and gas consumption. Although, this work advanced significantly the state-of-the-art, we can identify two main limitations. First, the authors considered this as an intrinsic property of the building, assuming an extremely dense small-cell network with antennas deployed throughout the entire building. That is commonly not the case, as MNOs choose to install only a limited number of small-cells per building. Second, and more importantly, in order to derive an analytical solution for their metrics, the authors used simplistic empirical models. However, the accuracy of these models can be mediocre, and they are also inadequate to capture particularities in the building design, such as the geometry layout or the type of the construction materials [5].

Instead, deterministic propagation models, such as ray-tracing, consider physics-based information of an indoor environment of interest in order to estimate the characteristics of the wireless channel [5]. Thus, it is anticipated that these models will have a pivotal role in the deployment of indoor small-cells for 5G and beyond systems [6], [7]. Indeed, ray-tracing can be considerably more accurate than empirical models, however this comes at the price of a higher computational complexity and long simulation times. That was one of the dominant factors that led the authors of [3], [4] to use empirical models to evaluate BWP. However, more recently, to overcome the computational cost limitations a significant effort has been made to couple ray-tracing simulators with machine learning (ML), and create standalone generalizable data-driven propagation models [8], [9], [10]. These models can replicate closely the results of a ray-tracer, with the distinct advantage of a significantly reduced computational time, as their predictions require only a few milliseconds to execute.

©2022 IEEE. Personal use of this material is permitted. Permission from IEEE must be obtained for all other uses, in any current or future media, including reprinting/republishing this material for advertising or promotional purposes, creating new collective works, for resale or redistribution to servers or lists, or reuse of any copyrighted component of this work in other works.

An important aspect of radio propagation in indoor environments that is neglected when using empirical models is the uncertainty related to the environment description. This uncertainty can be attributed to the lack of knowledge regarding the geometry itself or regarding the properties, i.e., the permittivity and the conductivity, of the construction materials that are found within the geometry [11]. Indeed, the permittivity and the conductivity can vary significantly according to the material composition and the environmental conditions [12], [13]. Remarkably, in [13] which provides an overview of material parameter measurement campaigns used to develop ITU-R Recommendations [14], the values reported for the relative permittiviy of concrete at a single frequency ranged from 3 to 9. Hence, the results provide by simulators that use these parameters, e.g., a ray-tracer, will be subject to uncertainty due to the randomness in the simulator's inputs. Consequently, uncertainty will be introduced to any compound features that depend on the results of the propagation solver, e.g., the BWP metrics. This uncertainty can be quantified using conventional uncertainty quantification (UQ) tools, e.g., Monte Carlo methods, or efficient approaches such as polynomial chaos expansions (PCE) [15], [16], [17].

In this paper we advance the state of the art in indoor wireless network planning via the following original contributions.

- We introduce novel metrics that enable the quantification of the indoor wireless network performance (IWNP). Our IWNP metrics account for the actual radio access infrastructure planning, hence overcoming the limitations of current deployment-agnostic definitions like BWP.
- We include the intrinsic uncertainty related to the material properties of the indoor environment into IWNP calculations, and express the IWNP metrics as stochastic quantities. This substantially improves the reliability of results over present approaches that only consider the layout of the indoor environment.
- We propose a computationally efficient model of the stochastic IWNP metrics, which relies on (i) a pre-trained data-driven propagation model [9] and (ii) construction of a stochastic solution via an expedient PCE-based representation. By doing so, our approach enhances prior works where the performance metrics were evaluated using simplistic empirical propagation models [3], [4].
- We demonstrate that our solution provides a rigorous and reliable characterization of IWNP. It yields results similar to that of a high-performance physics-based radio propagation ray-tracer [18], but with a substantially reduced computational time.

Ultimately, our work enables the fast derivation of statistical indoor performance, providing higher confidence and flexibility to wireless network engineers for network planning.

II. Proposed Method

A. Indoor Wireless Network Performance Metrics

In this subsection, we introduce a set of metrics that can be used for the evaluation of IWNP. We aim at providing compound measures which can be leveraged by wireless network engineers, and assist the optimal wireless network design. Likewise, these metrics can be used by civil engineers or architects to assess how wireless-friendly is a building under design and if a building layout facilitates wireless communication. Unlike [3], [4], where the BWP metrics were defined with respect to the open-space scenario, the IWNP metrics used in this work consider only the propagation characteristics within the building. This is primarily because we seek to quantify the performance of an indoor wireless network itself, rather than comparing it to the open-space propagation scenario.

To quantify IWNP, three metrics are considered in this work, aiming to characterize the aggregated network coverage and capacity. The first two are the the power, P_{eff}, and the interference effectiveness, I_{eff}. The power effectiveness quantifies the coverage and how the building layout facilitates the propagation of the electromagnetic waves, and consequently how strong is the received signal from the serving device. Let $P_t^{(i)}$ and $PL^{(i)}(\omega)$ be the transmitting power and the pathloss (PL) distribution for the i-th transmitting device (Tx), respectively. Note that the PL distribution is defined over all locations ω in the area Ω covered by the indoor environment of interest. The power effectiveness over Ω is then:

$$P_{eff} = \frac{1}{\Omega}\int_{\Omega} P_t^{(a(\omega))}/PL^{(a(\omega))}(\omega)w(\omega)d\omega \tag{1}$$

where $a(\omega) = \arg\max_{i\in A} P_t^{(i)}/PL^{(i)}(\omega)$ represents the strongest available signal at each point of the grid, selected from the set of all Txs, A, and $w(\omega)$ is a weighting function assuming values between 0 and 1. The intuition behind the use of $w(\omega)$ is that certain areas within the building might not be of interest, e.g., storage rooms or bathrooms, thus through $w(\omega)$ we can limit their contribution in the compound metric. Secondly, the interference effectiveness captures how the signals emitted from different Txs interact with each other, quantifying the received signal-to-interference-plus-noise ratio (SINR):

$$I_{eff} = \frac{1}{\Omega}\int_{\Omega} \frac{P_t^{(a(\omega))}/PL^{(a(\omega))}(\omega)}{\sum_{i\in\bar{a}(\omega)} P_t^{(i)}/PL^{(i)}(\omega) + N_{ch}} w(\omega)d\omega \tag{2}$$

where $\bar{a}(\omega)$ indicates the set that includes all Txs apart from $a(\omega)$, i.e., $\bar{a}(\omega) = \{A - a(\omega)\}$, and N_{ch} is the channel noise. Note that I_{eff} is a qualitative proxy for the throughput and it is independent of the actual 5G system configuration. The third metric is the throughput effectiveness, T_{eff}, which is estimated based on the SINR and provides a quantitative insight regarding the end-user quality of service:

$$T_{eff} = \frac{1}{\Omega}\int_{\Omega} T(\omega)w(\omega)d\omega \tag{3}$$

where $T(\omega)$ is the throughput achieved at each point of the building and, given the SINR and the 5G channel configuration, i.e., the channel bandwidth, modulation order, code rate, etc., that can be estimated from the 3GPP standards [19], [20].

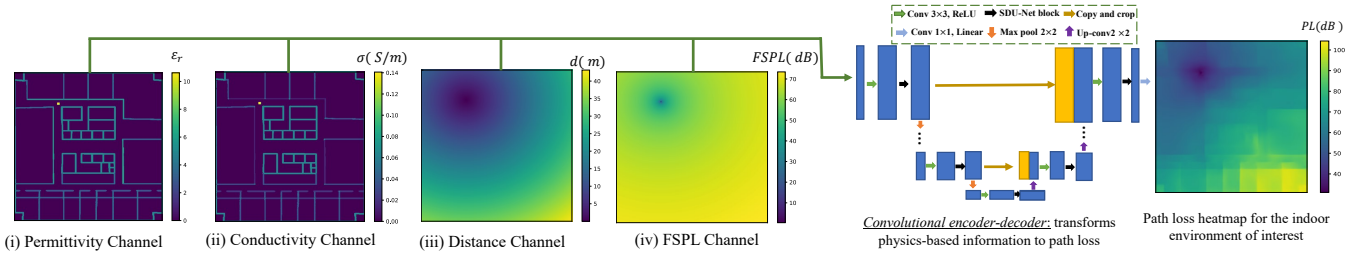


Fig. 1: Schematic of EM DeepRay [9].

To compute any of the IWNP metrics it is necessary to have a closed-form solution that describes the PL distribution over space. An exact solution of Maxwell's equations is practically infeasible: thus, in [3], [4] the authors estimated similar metrics by considering simplistic empirical propagation models, such as the multi-slope path gain model. However, the PL distribution can be readily derived from radio propagation solvers, such as a ray-tracer. Then, assuming a dense grid discretization, the integrals in (1) – (3) can be evaluated as a Riemann sum, where the summation terms are provided by the propagation solver.

B. EM DeepRay

Ray tracing has been widely used for wireless channel characterization, and although it can model precisely radio wave propagation, its main limitation is the high computational resources it requires. In particular, it is necessary to discretize the simulation domain, estimate intersections between rays and walls, trace ray paths, and determine all the rays that can reach a receiving point. That entails a substantial complexity and it can take minutes or even hours.

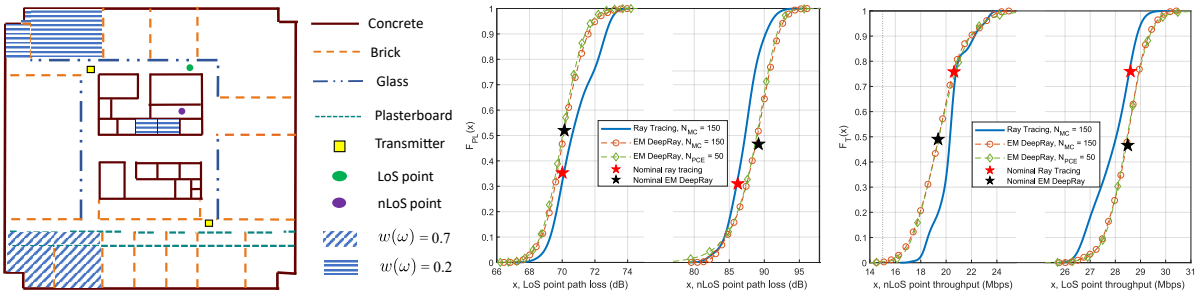
This issue has motivated the development of ML-based propagation models that can be trained with synthetic data derived from a high performance propagation solver [8], [9], [10]. Once trained, these models can be used to replicate much more rapidly the results of the propagation solver. In [9], a convolutional encoder-decoder was employed to encode physics-based information of an indoor environment and decode it as a PL heatmap. The proposed data-driven model, referred to as EM DeepRay, was trained with synthetic data created by conducting multiple ray tracing simulations at various indoor environments and operating frequencies. Eventually EM DeepRay learnt to recognize the details of a radio environment and it could predict the PL for unknown indoor geometries and frequency bands, not seen during the training phase, within a few milliseconds.

The input of EM DeepRay was a four-channel tensor, where the four channels depict: (i) the relative permitivity, ϵ_r, (ii) the conductivity, σ_c, of the building materials at each point of the simulated grid, (iii) the distance, d, between the transmitter and every point within the simulated grid, (iv) and the free space path loss (FSPL), assuming the building was absent. As shown in Fig 1, the input channels were concatenated and passed to a convolutional encoder-decoder, specifically a stacked dilated convolutions U-Net (SDU-Net) with its parameters set according to [9], which transformed the input tensor into a PL heatmap. The data-driven model was completely agnostic with respect to the laws of the electromagnetism, however, through training it was feasible to estimate proper weights that matched the physics-based information to the correct PL values. Hence, instead of estimating intersections between rays and walls, and tracing the ray paths, EM DeepRay estimates the PL for an indoor geometry though simple and fast weight matrix multiplications. Combining computational speed and high accuracy renders EM DeepRay an expedient and rigorous tool suitable for cases where multiple radio propagation simulations are required, e.g., when finding optimal network topology or for wireless channel uncertainty quantification.

C. Uncertainty Quantification

To estimate the strength and the phase of the waves reflected from and transmitted through building walls in ray-tracing simulators, it is necessary to compute the respective slab reflection and transmission coefficients based on the values of ϵ_r and σ_c [5]. In a similar manner, EM DeepRay infers the PL based on the values of the electromagnetic properties of the the construction materials depicted in the first two channels of the input tensor shown in Fig. 1. The values of ϵ_r and σ_c are typically derived from look-up tables of ITU standards [14], and they correspond to the median value estimated through large measurement campaigns. Thus, it is likely that the actual material parameter values in different scenarios can vary considerably from those reported in [14].

In fact, the material parameters should be treated as random variables following a certain probability density function (PDF) [11]. Consequently, all the physical quantities related to them, such as the PL distribution, should be considered as stochastic quantities. The common method to quantify the uncertainty for these stochastic quantities is the Monte Carlo approach that allows the evaluation of statistical parameters, such as the mean or the standard deviation, by conducting multiple runs of the same problem assuming different values of the input random variables. Despite its simplicity, the Monte Carlo approach exhibits a slow convergence rate, inversely proportional to the square root of the number of the problem runs [15]. Instead, a PCE-based representation of the stochastic quantity yields a faster and guaranteed convergence, providing an actual solution to the UQ problem [15]. In this case, the stochastic quantity, $X(\xi)$, is expanded to an orthogonal basis of polynomial functions [15]:



(a) Geometry under consideration.

(b) Path loss CDFs for LoS/nLos points.

(c) Throughput CDFs for LoS/nLos points.

Fig. 2: Geometry under consideration, along with the simulated PL and throughput CDFs for a LoS and nLos point.

$$X(\xi) = \sum_{k=0}^{P} u_k \Psi_k(\boldsymbol{\xi}) \tag{4}$$

where u_k are the coefficients of the basis functions, the input vector $\boldsymbol{\xi} = [\xi_1, \xi_2, ..., \xi_N]$ comprises the N input random variables, and Ψ_k are multi-variate polynomial basis functions, selected according to the PDF of the input random variables [16]. The number of the polynomials, P, used to represent the stochastic quantity is $P + 1 = (N + D)!/N!D!$, where D is the highest polynomial order taken into account [15].

The coefficients of the expansion in (4), can be computed through projection-based methods, such as the Smolyak sparse quadrature, or least-squares minimization methods, such as the orthogonal matching pursuit (OMP) algorithm [21]. The OMP algorithm creates a sparse representation of the PCE in (4), by considering only the terms with the highest contribution, and hence reducing the computational cost. Assuming N_{PCE} repetitions of a UQ problem, one can form an output matrix $\mathbf{Y} = [\mathbf{Y}^{(1)}, \mathbf{Y}^{(2)}, ..., \mathbf{Y}^{(N_{PCE})}]^\intercal$ including the deterministic responses of the stochastic quantity for each repetition. Similarly, an input matrix can be formed, $\boldsymbol{\Xi} = [\boldsymbol{\xi}^{(1)}, \boldsymbol{\xi}^{(2)}, ..., \boldsymbol{\xi}^{(N_{PCE})}]^\intercal$, where $\boldsymbol{\xi}^{(m)}$ denotes the sampled input random variables for the m-th repetition, and a matrix $\boldsymbol{\Psi}(\boldsymbol{\xi}^{(m)}) = [\Psi_0(\boldsymbol{\xi}^{(m)}), \Psi_1(\boldsymbol{\xi}^{(m)}), ..., \Psi_P(\boldsymbol{\xi}^{(m)})]$ containing the values of the orthogonal polynomials for each repetition. Then, the coefficients can be computed through:

$$\hat{\mathbf{u}} = \arg\min_{\mathbf{u}} \mathbb{E}[(\boldsymbol{\Psi}(\boldsymbol{\Xi})\mathbf{u}^\intercal - \mathbf{Y})^2] \tag{5}$$

where $\mathbf{u} = [u_0, u_1, ..., u_P]^\intercal$ is a vector containing all the PCE coefficients. The OMP algorithm searches and determines iteraively the polynomial basis functions with the highest contribution in the PCE [21]. Assuming that initially all the coefficients are zeroed, at each iteration, the algorithm selects the polynomial basis function that exhibits the highest correlation to the error metric, $\boldsymbol{R} = \boldsymbol{Y} - \boldsymbol{u}^\intercal \boldsymbol{\Psi}(\boldsymbol{\xi})$, and the coefficient of the basis functions is estimated through (5). Once the coefficients are estimated, the PCE constitutes a solution to the UQ problem, portraying the response of the stochastic quantity to some random inputs. In addition, the mean value and the standard deviation of the stochastic quantity can be then estimated as [15]:

$$\mu[X(\xi)] = u_0 \tag{6}$$

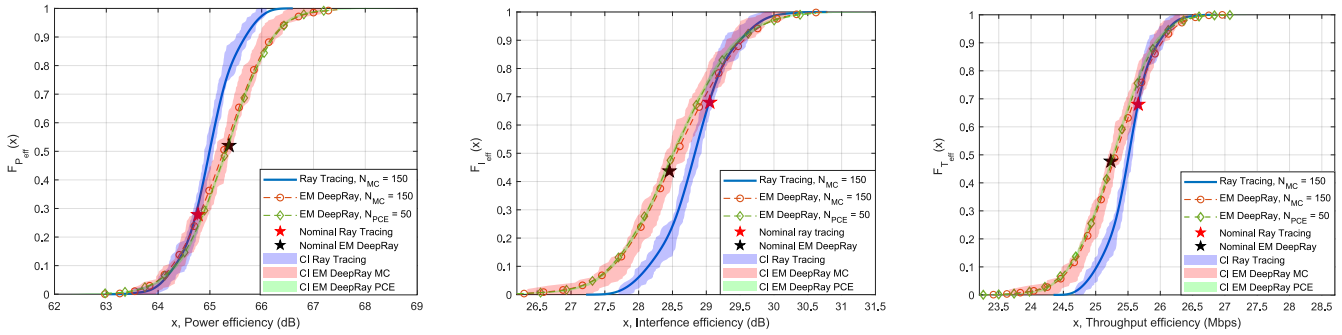
$$\sigma^2[X(\xi)] = \sum_{k=1}^{P} u_k^2 \langle {\Psi_k}^2(\xi) \rangle \tag{7}$$

III. Simulation Results

To demonstrate the proposed method, we generate the geometry shown in Fig. 2a, and we assume two Txs found within the building, depicted as yellow square boxes. Both Txs use antennas with an omnidirectional beam pattern, and their operating frequency is 2.6 GHz. The channel bandwidth is 5 MHz, the sub carrier spacing is 15 kHz, and the number of resource blocks is 25. The transmission power for both Txs is set to 0 dBm. Then, for each point within the simulated grid, we select the Tx with the strongest signal as the serving one, while we assume that the two Txs operate in a different channel and hence they do not interfere. We further assume a constant noise power spectral density equal to -174 dBm/Hz and a noise figure at the receiving signal chain equal to 5 dB.

The geometry comprises four different construction materials that are commonly found indoor environments: concrete, brick, glass and plasterboard. For each material we assume that its electric properties are random variables following the sampling distributions shown in Table I. The mean values of the sampling distributions correspond to the nominal values provided by [14]. We further assume a standard deviation approximately equal to 15% of the nominal value [11]. Hence, we have in total $N = 8$ random variables, ξ_i, depicting the uncertainty regarding the two fundamental electromagnetic properties of the four construction materials found within the geometry shown in Fig. 2a. Thus, the PL distribution, $PL(\omega)$ is a stochastic quantity depending on the material parameters, i.e., $PL(\omega, \boldsymbol{\xi})$, and consequently so are the IWNP metrics.

To quantify the uncertainty, we conduct $N_{MC} = 150$ ray tracing and EM DeepRay simulations assuming different values of ϵ_r and σ_c, drawn from the input sampling distributions of Table I using the Latin hypercube sampling method. The pre-trained EM DeepRay yielded an approximately 5 dB RMSE compared to the nominal values ray tracing simulation results. Thus, to have equivalent results in the UQ analysis, we calibrate the pre-trained model, as outlined in [9] to almost



(a) Power effectiveness CDFs and CIs. (b) Interference effectiveness CDFs and CIs. (c) Throughput effectiveness CDFs and CIs.

Fig. 3: CDFs and CIs of the various IWNP metrics for the indoor geometry shown in Fig. 2a.

match the results of the nominal ray tracing simulation, and then we run the 150 EM DeepRay UQ simulations.

TABLE I: INPUT SAMPLING DISTRIBUTIONS.

	Concrete	Brick	Glass	Plasterboard
ϵ_r	$\mathcal{N}(5.31, 0.66)$	$\mathcal{N}(3.75, 0.46)$	$\mathcal{N}6.27, 0, 78)$	$\mathcal{N}(2.94, 0.36)$
σ_c	$\mathcal{N}(0.070, 0.008)$	$\mathcal{N}(0.038, 0.004)$	$\mathcal{N}(0.013, 0.001)$	$\mathcal{N}(0.022, 0.002)$

Initially, we explore the impact of the input uncertainty on the simulated PL for a line-of-sight (LoS) and a non-line-of-sight (nLoS) point, which are depicted in Fig. 2a as a green and a purple dot, respectively. As we can see in Fig. 2b, where the PL for the nominal values of ϵ_r and σ_c is shown with an asterisk, the simulated PL can vary due to material parameter uncertainty. The statistics of the UQ analysis are presented in Table II. An interesting observation is that the uncertainty is higher for the nLoS point compared to that of the LoS point, since we can observe that the range of the PL fluctuation is considerably larger. That conforms with intuition, since for nLoS points there are multiple walls interposed between the receiver and the Tx, and thus PL is affected by multiple unknown parameters. Consequently, we calculate the throughput for these two points based on [19], and by mapping the estimated SINR to the modulation scheme and the coding rate according to the values reported in [20]. As we can see in Fig. 2c, the uncertainty in the PL also translates into variation of the estimated throughput. Hence, the randomness in the material parameters is also important from the perspective of the end-user, as it affects their quality of experience and service.

TABLE II: STATISTICS OF THE LOS AND NLOS POINT.

	$\mu \pm \sigma^2$		[min, max]	
	Ray Tracing	EM DeepRay	Ray Tracing	EM DeepRay
PL(LoS) (dB)	70.7 ± 1.4	70.1 ± 1.1	[68.3, 72.8]	[67.5, 73.1]
PL(nLos) (dB)	87.7 ± 2.1	88.8 ± 2.5	[81.8, 93.3]	[82.1, 92.8]
T(LoS) (Mbps)	27.8 ± 0.5	28.4 ± 0.4	[26.7, 29.1]	[26.4, 29.9]
T(nLos) (Mbps)	20.6 ± 1.6	19.4 ± 2.3	[17.1, 23.6]	[15.7, 23.5]

The distinct advantage of quantifying this randomness with a data-driven propagation model is the tremendously reduced computational time. A single ray tracing simulation requires 2-3 minutes per Tx, i.e., 4-6 minutes per simulation scenario. On the other hand, EM DeepRay can furnish estimates of the PL distribution for both Txs only within approximately half a second. Thus, conducting a UQ analysis with ray tracing can take up to 10 hours, whereas the same results can be derived with a data-driven model within approximately a minute. The expediency of EM DeepRay does not affect the quality of the results, since as we can observe from Figs. 2b and 2c, the cumulative distribution functions (CDFs) for the ray-tracer and EM DeepRay results yield a very good resemblance. We also observe that the stochastic solution generated from the PCE, with $N_{PCE} = 50$ samples and with highest polynomial order $D = 4$, yields the same CDF as Monte Carlo, however, the number of simulations required to converge is 3 times smaller.

Now that is evident that the uncertainty in ϵ_r and σ_c can affect radiowave propagation and the end-user's experience, we proceed with the evaluation of the IWNP metrics. We assume that within the building exist areas which are of lower wireless communication importance, e.g., toilets or storage rooms. Hence, for these areas we assign lower values to the weighting function, $w(\omega)$, in order to limit their contribution in the IWNP metrics. In particular, for the areas covered with diagonal and horizontal blue lines, the weighting functions is equal to 0.7 and 0.2, respectively. Since for both ray tracing and EM DeepRay we have a dense grid discretization, i.e., PL(ω) is evaluated once per 0.1 m, it is possible to approximate (1) – (3) numerically and accurately through a Riemann summation.

As we can see from Figs. 3a-3c, there is again a close correspondance between the CDFs provided by the ray-tracer and EM DeepRay either using the Monte Carlo method or a PCE-based representation. However, the construction of the stochastic solution through PCE requires only 50 EM DeepRay simulations, i.e., three times fewer than that of the Monte Carlo, whilst the estimation of the sparse PCE coefficients via OMP takes only one second. Additionally, the confidence intervals (CIs) estimated through a PCE representation are tight (visually invisible green area around the dashed green lines) compared to those calculated via the conventional Monte Carlo approach. The statistics of the IWNP metrics are shown in

Table III. As we can observe the mean, the standard deviation, as well as the minimum and the maximum values of the IWNP metrics estimated via ray tracing and EM DeepRay are almost the same. However, as mentioned earlier the UQ analysis of the IWNP metrics with EM DeepRay takes approximately a minute, whilst using ray tracing requires a couple of hours.

TABLE III: STATISTICS OF THE IWNP METRICS.

	$\mu \pm \sigma^2$		[min, max]	
	Ray Tracing	EM DeepRay	Ray Tracing	EM DeepRay
P_{eff} (dB)	64.9 ± 0.5	65.3 ± 0.7	[63.5, 66.1]	[63.4, 67.2]
I_{eff} (dB)	28.8 ± 0.5	28.5 ± 0.7	[27,7, 30,3]	[26.3, 30.3]
T_{eff} (Mbps)	25.5 ± 0.4	25.3 ± 0.5	[24.6, 26.5]	[23.6, 26.5]

Ultimately, our proposed method enables the accurate computation of stochastic IWNP metrics over all locations of a target indoor space in minutes or less. By dramatically reducing the execution time of this task, our method allows for testing a large number of potential radio access infrastructure deployments, which would not be bearable under previous approaches. Our work thus paves the way for an innovative approach to indoor wireless radio planning, which is fully data-driven, accounting for uncertainties in the propagation environment and yielding an optimized IWNP.

IV. CONCLUSION

In this paper we introduced metrics that can be used to quantify IWNP, and we highlighted how a data-driven propagation model can be leveraged for the robust and expedient evaluation of these metrics. The proposed evaluation method blends the accuracy of a high performance propagation solver with the computational efficiency of deep neural networks. On top of considering the physics of the environment of interest, our approach also accounts for the innate uncertainty that exists within the indoor geometry. To quantify the uncertainty, a stochastic solution was constructed through a PCE representation, enabling a faster convergence and the rigorous characterization of the IWNP metrics statistics. In the future, we seek to introduce more uncertainties and also explore how the IWNP metrics estimated by EM DeepRay can be exploited through stochastic optimization in order to identify the optimal network deployment under uncertainty.

ACKNOWLEDGMENT

This work was supported by the European Commission through the Horizon 2020 Framework Program, H2020-MSCA-ITN-2019, MSCA-ITN-EID, under Grant 860239, BANYAN

REFERENCES

[1] Cisco, "Cisco vision: 5G-thriving indoors [white paper]," 2017.
[2] M. Agiwal, A. Roy, and N. Saxena, "Next generation 5G wireless networks: A comprehensive survey," *IEEE Commun. Surveys Tuts.*, vol. 18, no. 3, pp. 1617–1655, 2016.
[3] J. Zhang, A. A. Glazunov, and J. Zhang, "Wireless performance evaluation of building layouts: Closed-form computation of figures of merit," *IEEE Trans. Commun.*, vol. 69, no. 7, pp. 4890–4906, 2021.
[4] J. Zhang, A. A. Glazunov, W. Yang, and J. Zhang, "Fundamental wireless performance of a building," *IEEE Wirel. Commun.*, 2021.
[5] T. K. Sarkar, Z. Ji, K. Kim, A. Medouri, and M. Salazar-Palma, "A survey of various propagation models for mobile communication," *IEEE Antennas Propag. Magazine*, vol. 45, no. 3, pp. 51–82, 2003.
[6] F. Fuschini, E. M. Vitucci, M. Barbiroli, G. Falciasecca, and V. Degli-Esposti, "Ray tracing propagation modeling for future small-cell and indoor applications: A review of current techniques," *Radio Science*, vol. 50, no. 6, pp. 469–485, 2015.
[7] D. He, B. Ai, K. Guan, L. Wang, Z. Zhong, and T. Kürner, "The design and applications of high-performance ray-tracing simulation platform for 5G and beyond wireless communications: A tutorial," *IEEE Commun. Surveys Tuts.*, vol. 21, no. 1, pp. 10–27, 2018.
[8] A. Seretis and C. D. Sarris, "Towards physics-based generalizable convolutional neural network models for indoor propagation," *IEEE Trans. Antennas Propag.*, 2022.
[9] S. Bakirtzis, J. Chen, K. Qiu, J. Zhang, and I. Wassell, "EM DeepRay: An expedient, generalizable and realistic data-driven indoor propagation model," *IEEE Trans. Antennas Propag.*, vol. 70, no. 6, pp. 4140–4154, 2022.
[10] S. Bakirtzis, K. Qiu, J. Zhang, and I. Wassell, "DeepRay: Deep learning meets ray-tracing," in *2022 16th European Conference on Antennas and Propagation (EuCAP)*, 2022.
[11] A. C. Austin, N. Sood, J. Siu, and C. D. Sarris, "Application of polynomial chaos to quantify uncertainty in deterministic channel models," *IEEE Trans. Antennas Propag.*, vol. 61, no. 11, pp. 5754–5761, 2013.
[12] S. Stavrou and S. Saunders, "Review of constitutive parameters of building materials," in *Twelfth International Conference on Antennas and Propagation, 2003 (ICAP 2003).(Conf. Publ. No. 491)*, vol. 1. IET, 2003, pp. 211–215.
[13] R. Rudd, K. Craig, M. Ganley, and R. Hartless, "Building materials and propagation," *Final Report, Ofcom*, vol. 2604, 2014.
[14] ITU-Rec, "Recommendation P.2040-1, Effects of building materials and structures on radiowave propagation above about 100 MHz," *Int. Telecommun. Union, Geneva, Switzerland*, 2015.
[15] O. Le Maitre and O. M. Knio, *Spectral methods for uncertainty quantification: with applications to computational fluid dynamics*. Springer Science & Business Media, 2010.
[16] D. Xiu, *Numerical methods for stochastic computations: a spectral method approach*. Princeton university press, 2010.
[17] S. Marelli and B. Sudret, "Uqlab: A framework for uncertainty quantification in matlab," in *Vulnerability, uncertainty, and risk: quantification, mitigation, and management*, 2014.
[18] (2021) Ranplan Wireless, Ranplan Professional. [Online]. Available: https://ranplanwireless.com/
[19] Access Evolved Universal Terrestrial Radio, "User equipment (UE) radio access capabilities," *Standard ETSI TS*, vol. 136, no. 306, p. V14, 2015.
[20] S. Sesia, I. Toufik, and M. Baker, *LTE-the UMTS long term evolution: from theory to practice*. John Wiley & Sons, 2011.
[21] S. Bakirtzis, X. Zhang, and C. D. Sarris, "Stochastic modeling of wave propagation in waveguides with rough surface walls," *IEEE Trans. Microw. Theory Techn.*, vol. 69, no. 1, pp. 500–508, 2020.